



# Compound-specific isotope analysis resolves the dietary origin of docosahexaenoic acid in the mouse brain<sup>S</sup>

R. J. Scott Lacombe,\* Vanessa Giuliano,\* Stefanie M. Colombo,<sup>†</sup> Michael T. Arts,<sup>†</sup> and Richard P. Bazinet<sup>1,\*</sup>

Department of Nutritional Sciences,\* Faculty of Medicine, University of Toronto, Toronto, Ontario M5S 3E2, Canada; and Department of Chemistry and Biology,<sup>†</sup> Ryerson University, Toronto, Ontario M5B 2K3, Canada

**Abstract** DHA (22:6n-3) may be derived from two dietary sources, preformed dietary DHA or through synthesis from  $\alpha$ -linolenic acid (ALA; 18:3n-3). However, conventional methods cannot distinguish between DHA derived from either source without the use of costly labeled tracers. In the present study, we demonstrate the proof-of-concept that compound-specific isotope analysis (CSIA) by GC-isotope ratio mass spectrometry (IRMS) can differentiate between sources of brain DHA based on differences in natural  $^{13}\text{C}$  enrichment. Mice were fed diets containing either purified ALA or DHA as the sole n-3 PUFA. Extracted lipids were analyzed by CSIA for natural abundance  $^{13}\text{C}$  enrichment. Brain DHA from DHA-fed mice was significantly more enriched ( $-23.32\text{‰}$  to  $-21.92\text{‰}$ ) compared with mice on the ALA diet ( $-28.25\text{‰}$  to  $-27.49\text{‰}$ ). The measured  $^{13}\text{C}$  enrichment of brain DHA closely resembled the dietary n-3 PUFA source,  $-21.86\text{‰}$  and  $-28.22\text{‰}$  for DHA and ALA, respectively. The dietary effect on DHA  $^{13}\text{C}$  enrichment was similar in liver and blood fractions. Our results demonstrate the effectiveness of CSIA, at natural  $^{13}\text{C}$  enrichment, to differentiate between the incorporation of preformed or synthesized DHA into the brain and other tissues without the need for tracers.—Lacombe, R. J. S., V. Giuliano, S. M. Colombo, M. T. Arts, and R. P. Bazinet. **Compound-specific isotope analysis resolves the dietary origin of docosahexaenoic acid in the mouse brain.** *J. Lipid Res.* 2017. 58: 2071–2081.

**Supplementary key words** fatty acid • stable isotope analysis • omega-3 fatty acids

DHA (22:6n-3) is the major n-3 PUFA within the brain, comprising over 10% of total brain FAs (1, 2). The incorporation of DHA into brain phospholipids serves to regulate the function and structural organization of neuronal membranes, as well as acting as a reservoir of substrate for the production of bioactive docosanoids and DHA-derived docosahexaenoyl ethanolamide (3). Several studies have demonstrated DHA and its enzymatically derived mediators to regulate neurogenesis, cell survival, synaptic function, and the resolution of neural inflammation (3–5). Despite the apparent critical role of DHA in these processes, the brain relies on an external supply of DHA, which can be sustained by either the provision of preformed DHA or through hepatic synthesis from  $\alpha$ -linolenic acid (ALA; 18:3n-3); however, there is still much debate surrounding the ability of ALA to solely sustain optimal tissue levels of DHA (6). As such, the study of DHA metabolism within the brain and other tissues is an area of ongoing research.

Commonly employed methods to study brain FA incorporation and metabolism in vivo involve the use of stable (e.g.,  $^2\text{H}$  or  $^{13}\text{C}$ ) or radio- (e.g.,  $^3\text{H}$  or  $^{14}\text{C}$ ) labeled tracers (7–13). Although these methodologies permit kinetic modeling of rates and turnovers for FAs involved in complex biological pathways, they are often associated with prohibitive costs, limiting studies to acute durations and singular dosing regimes. Typically, tracers are administered by oral gavage, intravenous bolus injections, or short steady-state infusions via cannulation, which in some instances can contribute to confounding levels of stress as well as limiting data collection to a metabolic snapshot. Notably, however, one study by Lefkowitz et al. (9) presented a novel approach whereby dietary ALA was replaced in its entirety with a  $^2\text{H}$ -labeled analog and fed to

This work was supported by Natural Sciences and Engineering Research Council of Canada Grant RGIN-2017-06465 to R.P.B. R.P.B. holds a Canada Research Chair in Brain Lipid Metabolism and has received research grants from Bunge Ltd., Arctic Nutrition, the Dairy Farmers of Canada, and Nestle Inc., as well as travel support from Mead Johnson and mass spectrometry equipment and support from Sciex. R.P.B. is on the executive committee of the International Society for the Study of Fatty Acids and Lipids and held a meeting on behalf of Fatty Acids and Cell Signaling, both of which rely on corporate sponsorship. R.P.B. has given expert testimony in relation to supplements and the brain. R.P.B. also provides complementary FA analysis for farmers, food producers, and others involved in the food industry, some of whom provide free food samples. V.G. holds a Canadian Institutes of Health Research Canada Graduate Scholarship.

Manuscript received 19 May 2017 and in revised form 5 July 2017.

Published, JLR Papers in Press, July 10, 2017  
DOI <https://doi.org/10.1194/jlr.D077990>

Abbreviations: ALA,  $\alpha$ -linolenic acid; ARA, arachidonic acid; CSIA, compound-specific isotope analysis; EA, elemental analyzer; FAME, fatty acid methyl ester; IRMS, isotope ratio mass spectrometry; LNA, linoleic acid; RBC, red blood cell; VPDB, Vienna PeeDee Belemnite.

<sup>1</sup>To whom correspondence should be addressed.

e-mail: richard.bazinet@utoronto.ca

<sup>S</sup> The online version of this article (available at <http://www.jlr.org>) contains a supplement.

rat pups over a 20 day period. Due to exorbitant costs associated with custom formulating a diet exclusively with an isotopically labeled tracer, it is reasonable to assume this approach is not likely to be replicated; thereby highlighting a demand for alternative cost effective techniques to study FA metabolism.

Elemental analysis by isotope ratio mass spectrometry (IRMS) may also be used at the level of natural isotopic enrichment to study the kinetics of carbon turnover (14–17). Resulting from enzymatic differences in carbon fixation pathways among  $C_3$  and  $C_4$  plants, a wide variation in natural abundance  $^{13}C$  enrichment exists within the food supply (18). Materials isolated from  $C_4$  plants are isotopically enriched (between  $-10\%$  and  $-16\%$ ) relative to material from  $C_3$  plants, which are more depleted in  $^{13}C$  (between  $-23\%$  and  $-32\%$ ). In addition, the fractionation of carbon isotopes in organisms from aquatic ecosystems differs slightly from  $C_3$  and  $C_4$  plants resulting, for example, in the tissues of marine fish ranging between  $-16\%$  and  $-22\%$  (19). Based on this well-characterized variation, natural abundance elemental carbon isotope analysis of human tissue has been used to distinguish between local dietary patterns; however, elemental analysis offers limited information on specific nutrients (19).

By pairing the resolving power of GC with the sensitivity of IRMS, compound-specific isotope analysis (CSIA) of  $^{13}C$  enrichment can be quantified for individual FAs (20, 21). Historically, the use of CSIA to study FA metabolism and kinetics has been applied almost exclusively to isotope tracer studies, with limited use at natural  $^{13}C/^{12}C$  abundance levels (22–26). With that said, however, applications of CSIA at the natural abundance level have demonstrated the assimilation of dietary FA  $^{13}C$  signatures ( $\delta^{13}C$ ) with plasma FAs, permitting the estimation arachidonic acid (ARA; 20:4n-6) and DHA synthesis (22, 23, 26). By supplementing infant formula with isotopically enriched DHA and ARA oils from microalgae as naturally occurring tracers, Carnielli et al. (26) adapted CSIA in a novel approach to measure the synthesis of long-chain PUFAs over several months. In addition, a similar approach has been used to estimate the contribution of DHA synthesis to muscle stores in rainbow trout (*Oncorhynchus mykiss*) fed a terrestrial ALA source for 12 weeks (27). CSIA, while currently underutilized in the study of human biology, presents a unique advantage over tracer studies by exploiting the innate variation in dietary  $^{13}C$  enrichment, permitting the study of FA metabolism in a chronic setting. Although advantageous over classical tracer studies in cost and permissible duration, CSIA has yet to be applied to study brain FA metabolism.

The purpose of the present study was to demonstrate the ability of CSIA, at natural  $^{13}C/^{12}C$  abundance levels, to distinguish between brain DHA synthesized endogenously from dietary ALA versus DHA obtained preformed from the diet. Although endogenously synthesized and preformed DHA are indistinguishable by conventional analytical methodologies,  $^{13}C$  isotopic signatures of precursor ALA and dietary DHA are measurably distinct based on natural  $^{13}C$  enrichment. Because DHA cannot be synthesized

de novo and must either be produced from the elongation and desaturation of ALA or consumed preformed, we predicted that brain  $\delta^{13}C_{DHA}$  signatures should indicate the relative incorporation and contribution of dietary n-3 PUFAs. Mice fed a diet containing either purified ALA or DHA as the only n-3 PUFAs, resulted  $\delta^{13}C_{DHA}$  signatures that were isotopically distinct. Furthermore,  $\delta^{13}C$  signatures of mouse brain DHA closely resembled  $\delta^{13}C$  signatures of the dietary n-3 PUFA source, either DHA or ALA. Our results highlight CSIA as an effective method to determine the dietary origin of DHA and, likely, other FAs.

## MATERIALS AND METHODS

### Materials

FA internal standards, heptadecanoic acid (17:0) and docosatrienoic ethyl ester (22:3n-3), along with GC reference mixes (GLC-569) were purchased from Nu Chek Prep Inc. (Elysian, MN). For isotopic analysis, reference materials, USGS70, USGS71, and USGS72, were obtained from the Reston Stable Isotope Laboratory-United States Geological Survey (Reston, VA). All solvents used were American Chemical Society or HPLC grade and were purchased from either Sigma-Aldrich (Mississauga, ON, Canada) or Fisher Scientific (Ottawa, ON, Canada). Boron trifluoride in methanol (14%) was purchased from Sigma-Aldrich. Purified ALA and DHA ethyl esters for dietary formulations were gifted from BASF Pharma Callanish Ltd. (Isle of Lewis, UK).

### Animals

All experimental protocols were approved by the Animal Ethics Committee at the University of Toronto and conducted in accordance to the policies and guidelines set forth by the Canadian Council on Animal Care and the Regulations of Animals for Research Act in Ontario (2016/2017 protocol number 20011661). Animals were housed within the University of Toronto Division of Comparative Medicine animal facility with ad libitum access to food and water in a temperature-controlled environment ( $21^{\circ}C$ ) featuring a 14 h/10 h light/dark cycle.

BALB/C 13–17-day-pregnant dams were ordered from Charles River Laboratories (Saint-Constant, Quebec, Canada), along with 6-week-old males (baseline). Upon arrival at the University of Toronto, pregnant dams were placed on diets containing either purified ALA or DHA at 2% of total FAs as the sole dietary n-3 PUFA. Offspring (F1 generation) were weaned onto the same diet as their respective dams. Female mice of the F1 generation maintained on purified n-3 PUFA diets were bred in-harem to produce the F2 generation. Male mice of the F1 and F2 generations were maintained on the purified n-3 PUFA diets of their dams until euthanization and tissue collection at 6 weeks of age. Mice were euthanized by cardiac puncture under terminal anesthesia with 2,2,2-tribromoethanol (Sigma-Aldrich) at 0.25 mg/g of body weight administered intraperitoneally. At the time of euthanization, tissues, including brain, liver, and blood fractions, were rapidly collected and flash-frozen in liquid nitrogen. All tissues were stored at  $-80^{\circ}C$  until the time of further processing.

### Diets

Purified n-3 PUFA diets were formulated from AIN-93 custom low n-3 rodent diet (Dyets, Inc., Bethlehem, PA). The diet contained, by weight, 10% fat, 60% carbohydrate, 20% protein, 5% fiber, and 5% vitamins/minerals/essential amino acids. Dietary lipids in the base rodent diet were derived from safflower,

hydrogenated coconut, and added oils (32.8, 63.2, and 4% by weight, respectively). Added oils were 2% oleate ethyl ester (Nu-Chek Prep Inc.) and either 2% ALA or 2% DHA ethyl ester (BASF Pharma Callanish Ltd.) as the only n-3 PUFA present in the diet, as confirmed by GC-flame ionization detection. The FA compositions of experimental diets were routinely measured in-house by GC-flame ionization detection in triplicate (Table 1, supplemental Fig. S1). Although the DHA ethyl ester used to formulate the DHA study diet was purified by HPLC, some residual ALA was nonetheless detected (0.06% total FA) in the DHA diet.

Purified ALA and DHA used to formulate the experimental diets were isolated from linseed and marine fish oils, respectively. The isotopic values of dietary ALA, DHA, and linoleic acid (LNA; 18:2n-6) were measured by CSIA, as described below (Table 1). The  $\delta^{13}\text{C}$  signatures of extracted dietary FAs both confirm the source of each FA, as the measured values are consistent with those of previous reports (28, 29), and indicate that the added oils are indeed foreign to the background oils used in each diet formulation, as they differ considerably from the isotopic values of other major FAs in the diets (data not shown).

### Lipid extraction and methylation

Lipids were extracted from brain, liver, and serum following methodologies adapted from Folch, Lees, and Sloane Stanley (30). Briefly, thawed samples of a given mass were homogenized and vortexed in 6 ml of 2:1 chloroform:methanol (by volume) in the presence of known quantities of heptadecanoic acid (17:0) and docosatrienoic ethyl ester (22:3n-3) as internal standards. Following 24 h at  $-20^\circ\text{C}$ , samples were brought to room temperature and 1.6 ml of 0.88% potassium chloride aqueous buffer were added followed by centrifugation at 500 g for 10 min at  $4^\circ\text{C}$  to impart organic phase separation. The lower organic phase containing chloroform and dissolved lipids was then transferred to a clean labeled glass tube and the remaining aqueous phase was washed with 4 ml of chloroform, vortexed, and centrifuged. The lower chloroform phase was then transferred and combined with the previously extracted phase.

Red blood cells (RBCs) were extracted similarly to the methods of Reed et al. (31). RBCs were weighed into test tubes containing 1 ml of chilled methanol and a known amount of internal standard, following which samples were immediately vortexed. One milliliter of chloroform was added and RBCs were held at  $-80^\circ\text{C}$

overnight. Samples were then brought to room temperature, vortexed vigorously, and centrifuged at 2,750 rpm for 5 min. Supernatants were collected into clean tubes and pellets were re-extracted with 2 ml of 1:1 chloroform:methanol (by volume). After combining extracts, 1.8 ml of 0.88% potassium chloride aqueous buffer were added and samples were centrifuged at 500 g for 10 min. The bottom chloroform was collected into a clean glass tube. All total lipid extracts were evaporated under nitrogen, reconstituted with a known volume of chloroform, and stored at  $-80^\circ\text{C}$  until methylation.

All samples were transesterified using methods adapted from Morrison and Smith (32). A portion of the total lipid extract was evaporated under nitrogen. Following evaporation, dried lipids were dissolved in 300  $\mu\text{l}$  of hexane to which 1 ml of 14% boron trifluoride in methanol was added and samples were heated at  $100^\circ\text{C}$  for 1 h. The transesterification of FAs in the presence of excess alcohol and an appropriate catalyst normally proceeds quantitatively; therefore, this method should not be expected to produce any kinetic isotope effect in the generation of FA methyl esters (FAMES) (33). The resulting FAMES were extracted into 1 ml of hexane, evaporated under nitrogen, and transferred into autosampler vials. Samples were diluted in hexane to a final concentration of approximately 0.5 mg of lipid per milliliter of solvent.

### Fatty acid quantification

FAMES were quantified on a Varian 430 gas chromatograph (Bruker, Billerica, MA) equipped with a SP-2560 100 m  $\times$  0.25 mm internal diameter  $\times$  0.20  $\mu\text{m}$   $d_f$  nonbonded poly (biscyanopropyl siloxane) capillary column (Supelco by Sigma-Aldrich, Bellefonte, PA) with He carrier gas at a constant flow rate of 3.0 ml/min. Samples (1  $\mu\text{l}$ ) were injected in splitless injection mode into a heated injection port held at  $250^\circ\text{C}$  via a Varian CP-8400 autosampler. FAMES were eluted using an oven temperature program initially set at  $60^\circ\text{C}$  and held for 2 min, increasing at  $10^\circ\text{C}/\text{min}$  to  $170^\circ\text{C}$ , and held for 4 min, then at  $6.5^\circ\text{C}/\text{min}$  to reach  $175^\circ\text{C}$ , then  $2.6^\circ\text{C}/\text{min}$  to reach  $185^\circ\text{C}$ , then  $1.3^\circ\text{C}/\text{min}$  to reach  $190^\circ\text{C}$ , and then  $8.0^\circ\text{C}/\text{min}$  to  $240^\circ\text{C}$  and held for 11 min. FAMES were detected by a flame ionization detector held at  $300^\circ\text{C}$ , operating at a sampling frequency of 20 Hz. Peaks were identified by retention time in comparison to an external reference standard mixture (GLC-569; Nu-Chek Prep Inc.). FAMES were quantified by dividing peak area under the curve by the 22:3n-3 internal standard area under the curve, then correcting for extracted tissue weight.

### Isotopic analysis

CSIA of isolated FAMES was carried out by GC-IRMS. FAMES (2  $\mu\text{l}$ ) were injected in splitless mode using a TriPlus RSH autosampler (Thermo Scientific, Bremen, Germany) onto a SP-2560 capillary column (Supelco) affixed in a Trace 1310 GC (Thermo Scientific). To achieve an adequate DHA signal, RBC samples were concentrated to 1 mg lipid per milliliter of hexane.

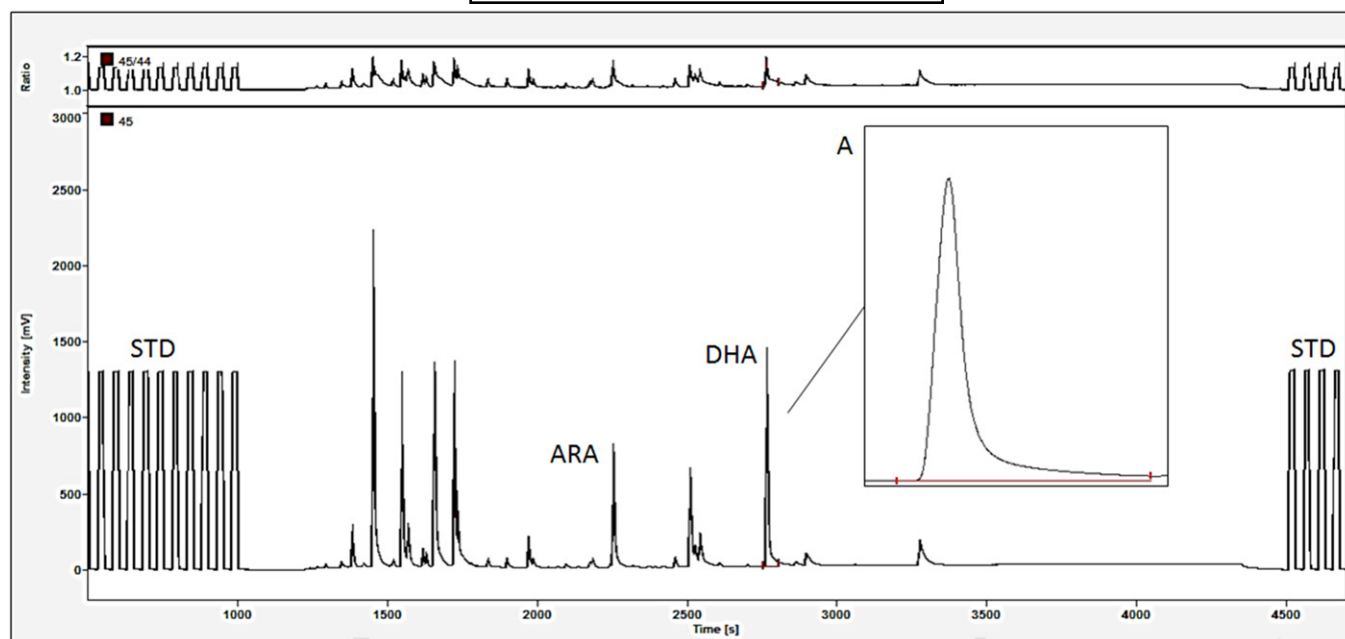
Partial integration due to improper oven temperature programs and peaking tail seriously compromises the accuracy and repeatability of the isotope ratio data measured by GC-IRMS. Therefore, complete resolution of the analyte of interest from surrounding peaks is imperative for high-precision CSIA (21). Complete baseline separation of DHA (Fig. 1) from surrounding peaks was achieved by the following temperature ramp: initial temperature of  $60^\circ\text{C}$  held for 2 min, increasing at  $10^\circ\text{C}/\text{min}$  to  $170^\circ\text{C}$  and held for 4 min, then at  $6.5^\circ\text{C}/\text{min}$  to  $175^\circ\text{C}$ , then  $2.6^\circ\text{C}/\text{min}$  to  $185^\circ\text{C}$ , then  $1.3^\circ\text{C}/\text{min}$  to reach  $190^\circ\text{C}$ , and then  $2.0^\circ\text{C}/\text{min}$  to  $240^\circ\text{C}$  and held for 11 min. Individual FAMES eluting off of the column were directed by He carrier gas to a GC Iso Link II combustion interface (Thermo Scientific) operating at

TABLE 1. Composition of major FAs in study diets

Fatty Acid	Relative Percent Fatty Acid	
	ALA	DHA
10:0	6.35 $\pm$ 0.04	6.50 $\pm$ 0.02
12:0	33.25 $\pm$ 0.17	33.36 $\pm$ 0.10
14:0	12.13 $\pm$ 0.03	11.82 $\pm$ 0.02
16:0	8.03 $\pm$ 0.00	8.02 $\pm$ 0.03
18:0	7.27 $\pm$ 0.03	7.65 $\pm$ 0.03
SFAs	67.39 $\pm$ 0.21	67.73 $\pm$ 0.10
18:1n-7	0.23 $\pm$ 0.01	0.23 $\pm$ 0.00
18:1n-9	7.27 $\pm$ 0.07	7.10 $\pm$ 0.03
MUFAs	7.59 $\pm$ 0.10	7.42 $\pm$ 0.01
18:2n-6	23.11 $\pm$ 0.11	23.07 $\pm$ 0.06
$\delta^{13}\text{C}_{18:2n-6}$	-30.44 $\pm$ 0.16‰	-30.77 $\pm$ 0.14‰
n-6	23.11 $\pm$ 0.11	23.14 $\pm$ 0.07
18:3n-3	1.91 $\pm$ 0.02	0.06 $\pm$ 0.00
$\delta^{13}\text{C}_{18:3n-3}$	-28.22 $\pm$ 0.29‰	—
22:6n-3	ND	1.65 $\pm$ 0.03
$\delta^{13}\text{C}_{22:6n-3}$	—	-21.86 $\pm$ 0.19‰
n-3	1.91 $\pm$ 0.02	1.71 $\pm$ 0.03

All values are mean  $\pm$  SD. Diets were measured in triplicate. ND, nondeterminable; SFA, saturated FA.





**Fig. 1.** GC-IRMS trace of FAMES derived from a mouse brain total lipid extract. The upper plot shows the signal ratio for  $m/z$  45/44. The lower plot shows the signal for  $m/z$  45 for the duration of the IRMS run. The exploded peak (A) highlights the complete baseline resolution of DHA from surrounding peaks. “STD” indicates signal peaks from the admitted calibrating  $\text{CO}_2$  reference gas; >10 pulses of calibrant were admitted prior to each run.

1,000°C with Ni and Cu wire catalysts. Compounds entering the combustion reactor were quantitatively combusted to  $\text{CO}_2$  and water. Water produced was trapped by a Nafion<sup>®</sup> dryer (DuPont, Wilmington, DE) and only pure  $\text{CO}_2$  was introduced into the Delta V Plus IRMS (Thermo Scientific) via a ConFlo IV (Thermo Scientific) continuous flow interface.

For elemental carbon isotopic analysis, a known amount sample was transferred into tin capsules and allowed to dry overnight at ambient temperatures. Extra care was taken to avoid environmental contamination of capsules and samples contained within, as elemental analyzer (EA) IRMS does not distinguish between carbon derived from the sample or from contamination (fingerprints, dust, oils, etc.). Capsules containing dry samples were introduced to a Flash 2000 elemental analyzer (Thermo Scientific) via a closed carousel Zero Blank autosampler (Costech Analytical Technologies Inc., Valencia, CA). The EA oxidation furnace ( $\text{Cr}_2\text{O}_3$  catalyst) and reduction furnace (Cu catalyst) were operated at 1,020°C and 650°C, respectively. Gases were routed to the IRMS via the above-mentioned interface. An automated correction for atmospheric  $\text{CO}_2$  was applied to each sample using data gathered from the combustion of a blank capsule prior to each daily run. Isodat Workspace version 3.0 (Thermo Scientific) was used for semi-automated processing of IRMS chromatograms.

Analytical error was measured with routine periodic injection of certified 20-carbon FAME reference materials (Reston Stable Isotope Laboratory) during every sequence. Error was determined to be  $\delta^{13}\text{C}_{\text{SD}} \leq 0.3\text{‰}$ , and was found to be within manufacturer specifications and similar to the values of those previously reported (22, 34, 35).

### Isotopic normalization

Carbon isotopic data collected by IRMS was normalized and reported as per mil (‰; 1‰ = 0.001 = 1 millurey or mUr) (36). Raw  $\delta^{13}\text{C}$  isotopic values obtained relative to the  $\text{CO}_2$  working gas (>10  $\text{CO}_2$  calibrant pulses during each run, see Fig. 1), from both GC-IRMS and EA analyses, were converted to the international carbon isotope reference scale, Vienna Pee Dee Belemnite (VPDB),

by multi-point linear normalization (37). Certified calibrated 20-carbon FAME reference materials, USGS70, USGS71, and USGS72, were injected periodically during each programmed sequence, totaling at least three injections per standard per run. Linear regression of measured versus true values ( $-30.53 \pm 0.04\text{‰}$ ,  $-10.50 \pm 0.03\text{‰}$ , and  $-1.54 \pm 0.03\text{‰}$  for USGS70, USGS71, and USGS72, respectively) was used to generate a normalizing equation, which was subsequently applied to report true  $\delta^{13}\text{C}$  values for all data (Fig. 2).  $R^2$  values for all normalizing equations were >0.998.

### Methylation correction

Isotopic analysis by GC-IRMS provides data on  $\text{CO}_2$  produced from the combustion of individual FAMES and, therefore, measurements include the contribution of carbon from the derivatized methyl group. To account for the contribution of the derivatized carbon, the following balance equation (equation 1) was used to correct all FA  $\delta^{13}\text{C}$  values:

$$n_{\text{FAME}}\delta^{13}\text{C}_{\text{FAME}} = \delta^{13}\text{C}_{\text{ME}} + n_{\text{FA}}\delta^{13}\text{C}_{\text{FA}} \quad (\text{Eq. 1})$$

where  $n$  refers to the number of moles of carbon and the subscripts, FAME, ME, and FA, refer to measured values of FAMES, derivatized methyl group, and FA, respectively. The isotopic value of the methyl group was determined using an EA to establish  $\delta^{13}\text{C}$  values for free and derivatized heptadecanoic acid (17:0; Nu-Chek Prep Inc.). Equation 1 was rearranged to solve for the isotopic value of the derivatized methyl group ( $\delta^{13}\text{C}_{\text{ME}}$ ) (equation 2).

$$\delta^{13}\text{C}_{\text{ME}} = n_{\text{FAME}}\delta^{13}\text{C}_{\text{FAME}} - n_{\text{FA}}\delta^{13}\text{C}_{\text{FA}} \quad (\text{Eq. 2})$$

where  $n$  is the number of moles of carbon and subscripts, FAME and FA, respectively correspond the derivatized and free FA. The value of the derivatized methyl carbon was determined to be  $-46.9\text{‰}$ . This value was used to correct all FAME data to generate true  $\delta^{13}\text{C}$  signatures for FAs.

## USGS 70,71,72 - Normalization Curve

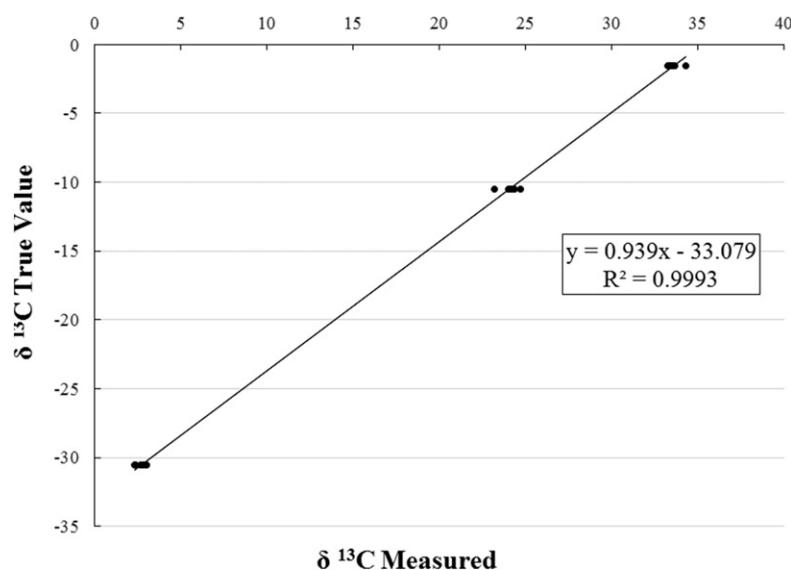


**Fig. 2.** Multipoint normalization curve for the reporting of true  $\delta^{13}\text{C}$  values for GC-IRMS data. FAME (20-carbon) certified reference materials, USGS70, USGS71, and USGS72, were injected periodically during each programmed sequence, totaling at least three injections per run.

### Discrimination factor calculation

Discrimination factors between diet and the brain were calculated by subtracting the  $\delta^{13}\text{C}$  signature of the dietary FA from the  $\delta^{13}\text{C}$  signature for brain DHA and ARA of each individual mouse. Dietary  $\delta^{13}\text{C}_{\text{ALA}}$  signatures were used in the case of the ALA-fed group, while  $\delta^{13}\text{C}_{\text{LNA}}$  signatures were used to calculate the discrimination factor for brain ARA.

### Statistics

All data are expressed as mean  $\pm$  SD. Sample sizes ranged between five and six mice per group. Brain, liver, serum, and RBC FA concentrations and  $\delta^{13}\text{C}$  signatures were compared using a two-way ANOVA to evaluate main and interaction effects of diet  $\times$  generation, with a Bonferroni post hoc test applied where there was a significant interaction effect. The level of significance is  $P < 0.05$ . All analyses were performed using GraphPad Prism (version 6.01; GraphPad Software Inc., La Jolla, CA).

## RESULTS

### FA tissue concentrations

After feeding mice purified ALA and DHA diets over two generations, there were no significant diet  $\times$  generation (F1 and F2) interaction effects ( $P > 0.05$ ) in brain, liver, and RBCs with respect to DHA concentrations (**Fig. 3**); however, serum concentrations did trend toward significance ( $P = 0.0614$ ).

In the absence of an interaction, there was a significant main effect of diet on DHA concentrations in brain, liver, serum, and RBCs ( $P > 0.001$  across all tissues). DHA concentrations were between 40% and 60% lower across serum, RBCs, and liver tissues in mice maintained on the ALA diet when compared with the DHA-fed group. Differences in DHA concentrations between mice fed either ALA or DHA diets were much less pronounced (**Fig. 3A**) in brain FAs for F1 ( $16.6 \pm 0.3 \mu\text{mol/g}$  vs.  $18.0 \pm 0.3 \mu\text{mol/g}$ , respectively) and F2 ( $16.8 \pm 0.3 \mu\text{mol/g}$  vs.  $18.4 \pm 0.5 \mu\text{mol/g}$ , respectively) generations.

There were no significant generational effects on DHA concentrations in brain, liver, and RBCs, with the serum DHA pool being the singular exception ( $P = 0.0169$ ).

Similar to DHA, there was no significant diet  $\times$  generation interaction effect with respect to ARA concentrations in any of the analyzed tissue (**Fig. 4**). However, there was a consistent main effect of diet across all tissues ( $P < 0.001$ ) such that ARA concentrations were higher in mice on the ALA diet compared with mice on the DHA diet. Differences in ARA concentrations between dietary groups were most pronounced in serum and liver, where levels were approximately 100% and 60% higher, respectively, in ALA-fed mice. Brain ARA concentrations were  $10.5 \pm 0.1 \mu\text{mol/g}$  and  $9.8 \pm 0.2 \mu\text{mol/g}$  in the F1 generation and  $10.5 \pm 0.3 \mu\text{mol/g}$  and  $10.0 \pm 0.4 \mu\text{mol/g}$  in the F2 generation for ALA and DHA diets, respectively. The differences in tissue ARA concentrations between dietary groups were independent of dietary LNA concentrations, as they did not differ between diets (Table 1).

### Isotopic signatures

Dietary effects of ALA and DHA diets on tissue  $\delta^{13}\text{C}_{\text{DHA}}$  signatures are presented in **Fig. 5**. The natural abundance  $\delta^{13}\text{C}$  of dietary n-3 PUFAs differed by 6.36‰ (Table 1), which was reflected in tissue  $\delta^{13}\text{C}_{\text{DHA}}$  signatures. There was no significant diet  $\times$  generation interaction effect on  $\delta^{13}\text{C}_{\text{DHA}}$  values in liver, serum, or RBCs; however, there was a significant main effect of diet on  $\delta^{13}\text{C}_{\text{DHA}}$  values in these tissues ( $P < 0.0001$ ). DHA from ALA-fed mice was found to be consistently more depleted in  $^{13}\text{C}$  when compared with that isolated from the DHA group. When pooling both generations, mean  $\delta^{13}\text{C}_{\text{DHA}}$  levels in liver, RBCs, and serum ranged between  $-28.33\text{‰}$  to  $-25.45\text{‰}$  and  $-22.71\text{‰}$  to  $-21.23\text{‰}$  for ALA- and DHA-fed mice, respectively. The measured differences in tissue  $\delta^{13}\text{C}_{\text{DHA}}$  between dietary groups clearly distinguish between the incorporation of either preformed or synthesized DHA.

With regard to brain  $\delta^{13}\text{C}_{\text{DHA}}$  signatures, there was a significant diet  $\times$  generation interaction effect ( $P = 0.001$ ).

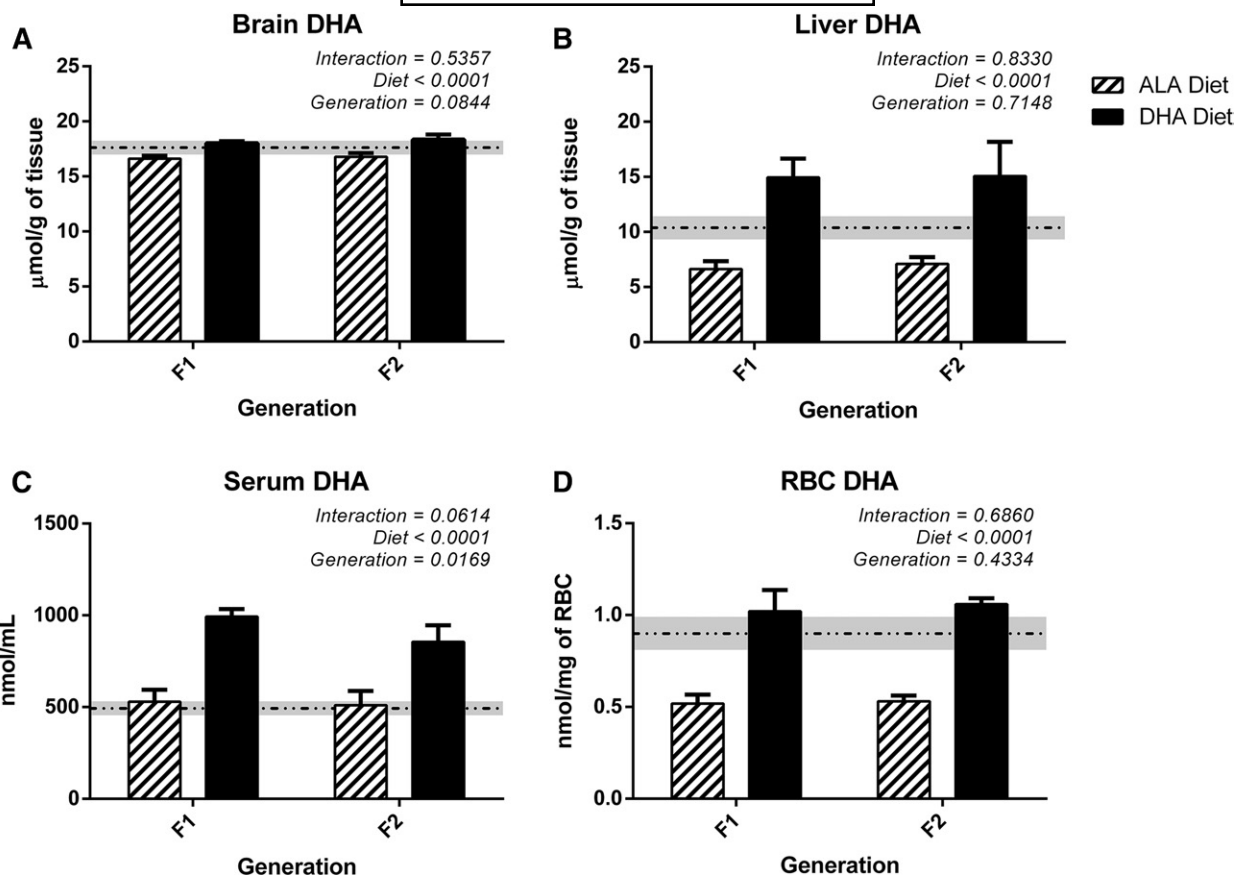


**Fig. 3.** DHA tissue concentrations of mice maintained on purified n-3 PUFA-containing diets over multiple generations. DHA concentrations were consistently higher in brain (A), liver (B), serum (C), and RBCs (D) of mice maintained on the DHA diet. All data are mean  $\pm$  SD ( $n = 5$ –6 per group). Data were compared by two-way ANOVA for the interaction of diet and generation; results are presented within each figure. The dashed line represents the mean DHA concentrations of baseline mice; the gray band indicates SD.

Post hoc analysis revealed that brain  $\delta^{13}\text{C}_{\text{DHA}}$  signatures in DHA-fed mice were significantly more enriched in  $^{13}\text{C}$  in comparison to the ALA diet group across both generations. In addition, DHA in the brains of the F2 generation mice were significantly more enriched in  $^{13}\text{C}$  than the DHA in brains of the F1 generation mice (Fig. 5A).

Dietary LNA  $\delta^{13}\text{C}$  signatures varied little between ALA and DHA diets (Table 1). There was no significant effect of dietary exposure on brain  $\delta^{13}\text{C}_{\text{ARA}}$  (Fig. 6A); however, there was a significant diet  $\times$  generation effect in liver and RBC  $\delta^{13}\text{C}_{\text{ARA}}$  values (Fig. 6B, D). Post hoc analysis of liver  $\delta^{13}\text{C}_{\text{ARA}}$  values found a significant 3% increase in  $^{13}\text{C}$  enrichment in F1 generation mice fed the DHA diet compared with the ALA group ( $-29.02 \pm 0.24\text{‰}$  and  $-29.81 \pm 0.49\text{‰}$ , respectively). There was no significant effect of diet or generation on RBC  $\delta^{13}\text{C}_{\text{ARA}}$  following post hoc analysis. While there was no significant interaction effect on serum  $\delta^{13}\text{C}_{\text{ARA}}$  signatures, there was a significant ( $P < 0.0001$ ) main effect by diet on serum  $\delta^{13}\text{C}_{\text{ARA}}$  signatures (Fig. 6C).

#### Brain isotopic discrimination factor

Mean brain isotopic discrimination factors between brain ARA and dietary LNA ranged between 1.73 and 2.40‰ (Fig. 7); there was no significant effect of diet or generation on this parameter (Fig. 7). A significant interaction effect ( $P = 0.001$ ) was observed with respect to the

brain DHA isotopic discrimination factor. Discrimination factors between ALA and DHA diets were found to be significantly different for F1 ( $0.39 \pm 0.33\text{‰}$  and  $-1.15 \pm 0.24\text{‰}$ ,  $P < 0.05$ ) and F2 ( $0.23 \pm 0.23\text{‰}$  and  $-0.37 \pm 0.28\text{‰}$ ,  $P < 0.05$ ) generations, respectively (Fig. 7). Within the DHA diet group, the F2 discrimination factor was 68% smaller than that of the F1 generation ( $P < 0.05$ ).

#### DISCUSSION

In the present study, we successfully discriminated, by CSIA, between brain DHA derived from terrestrial ALA and preformed marine DHA in adult mice maintained on purified n-3 PUFA-containing diets based solely on differences in natural abundance  $\delta^{13}\text{C}$  signatures. Brain  $\delta^{13}\text{C}_{\text{DHA}}$  signatures for mice maintained on ALA and DHA diets ranged between  $-28.25\text{‰}$  to  $-27.49\text{‰}$  and  $-23.32\text{‰}$  to  $-21.92\text{‰}$ , respectively, and closely resembled those of their respective dietary n-3 PUFA (Table 1). Additionally, the lack of any significant effect of dietary LNA on brain  $\delta^{13}\text{C}_{\text{ARA}}$  signatures between dietary groups further validates that the former result was driven by the  $\delta^{13}\text{C}$  signature of the origin n-3 PUFA. To the best knowledge of the authors, this represents the first time that CSIA was applied, at the natural abundance level, to distinguish between the incorporation of synthesized or preformed DHA into brain FAs.

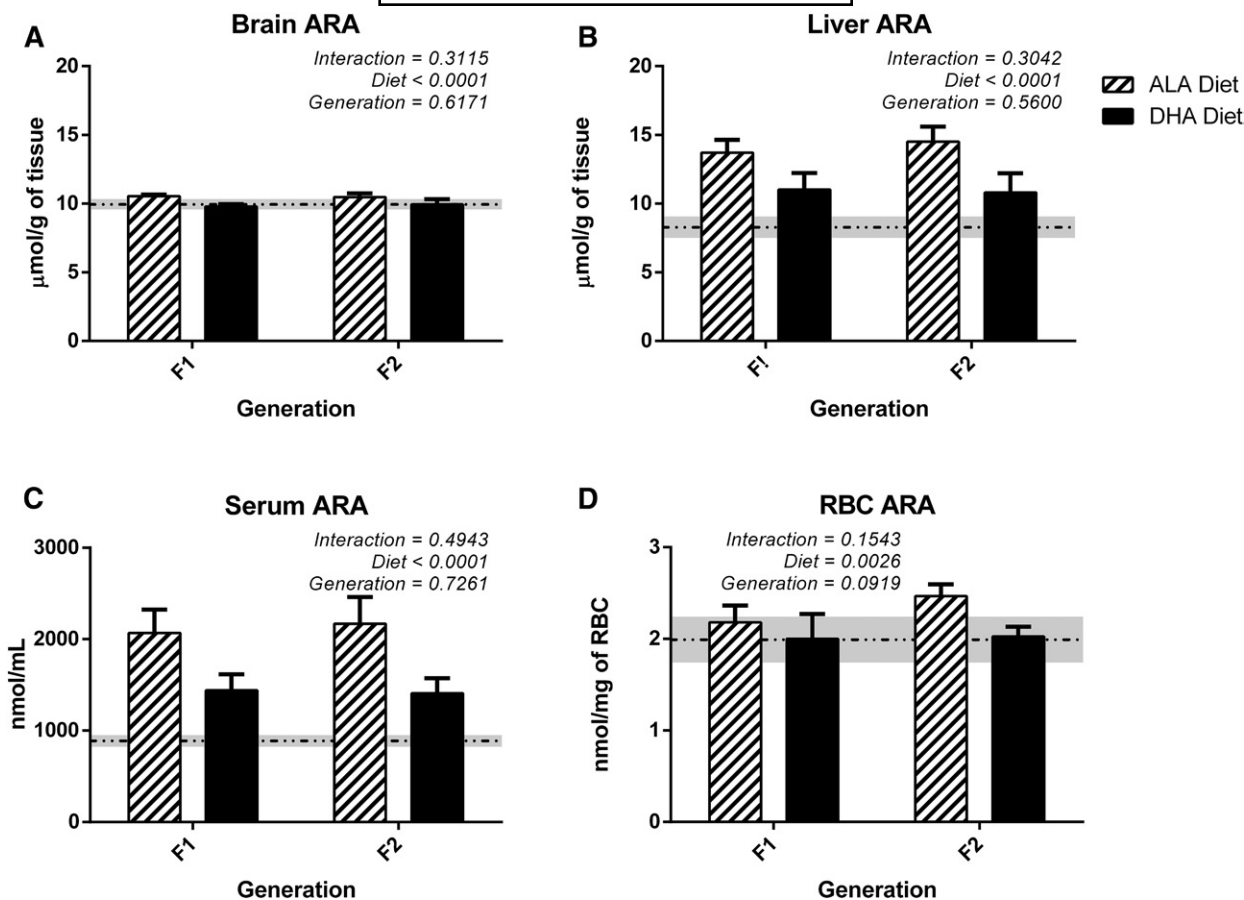


**Fig. 4.** ARA tissue concentrations of mice maintained on purified n-3 PUFA-containing diets over multiple generations. ARA concentrations were consistently lower in brain (A), liver (B), serum (C), and RBCs (D) of mice maintained on the DHA diet. All data are mean  $\pm$  SD ( $n = 5$ –6 per group). Data were compared by two-way ANOVA for the interaction of diet and generation; results are presented within each figure. The dashed line represents the mean ARA concentrations of baseline mice; the gray band indicates SD.

In the present study, we found mice fed preformed DHA to have approximately 8% higher brain DHA compared with those fed the 2% ALA diet, despite larger increases in circulating DHA ( $\sim 100\%$ ). The discrepancy between differences in blood and brain DHA levels were similar to those previously reported in rats consuming similar diets (38). While not addressed in the current experiment, it is unlikely that the higher brain DHA concentrations observed in the DHA-fed group would translate into measurable differences in behavioral or cognitive scores over the ALA fed group. Studies evaluating the effects of brain DHA on behavior and memory typically compare adequate versus complete, or near complete, n-3 PUFA deficiency, which, depending on the length of dietary exposure, may result in depletion of brain DHA by 30–80% (39–42). Furthermore, feeding of a 2% ALA diet likely fulfills the brain's basal requirement for DHA, as brain DHA levels remain constant down to  $\leq 0.8\%$  ALA and whole-body synthesis secretion rates of DHA from dietary ALA exceed the brain DHA uptake rate (38, 43).

Although the present study clearly demonstrated a significant effect of diet on brain  $\delta^{13}\text{C}_{\text{DHA}}$  signatures, there was also an apparent generational effect of the DHA diet. The redistribution and contribution of peripheral DHA stores established in utero to brain DHA has been reported

in newly born rat pups fed labeled-ALA formula for 20 days (9, 44). Although animals in the present study were maintained on study diets over multiple generations, there was a significant enrichment of 0.78‰ in the brain DHA of F2 mice compared with F1 mice on the DHA diet. This indicates some degree of incorporation from residual maternal DHA within the F1 generation, likely in peripheral stores established during the gestational period prior to the introduction of study diets.

Interestingly, however, there was an absence of a generational effect within the F1 and F2 mice on the ALA diets. We suggest that this may be an effect of the ALA diet on the FA content of milk and the resulting contribution to offspring stores established during lactation. Milk from lactating dams responds rapidly and selectively to changes in dietary exposure. Following 7–9 days on a DHA-containing diet, breast milk DHA content was 35% higher than mice fed a control diet containing ALA as the only n-3 PUFA (45). Therefore, offspring of mice fed ALA during lactation are likely to accumulate significantly lower DHA adipose stores during this period. Furthermore, feeding long-chain PUFA-free formula during neonatal development upregulates the tissue accretion of precursor-derived DHA (13). Given the significant contribution of peripheral DHA redistribution to brain DHA levels during development, we



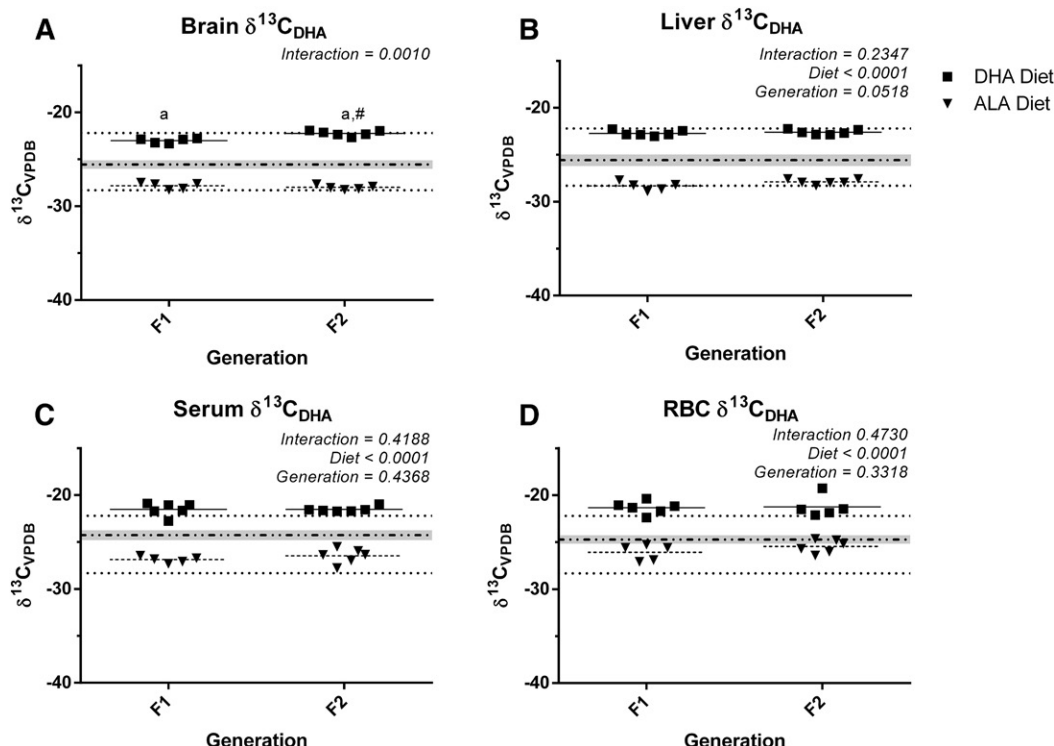


**Fig. 5.** DHA carbon isotope signatures of mice maintained on purified n-3 PUFA-containing diets over multiple generations. Brain (A), liver (B), serum (C), and RBC (D)  $\delta^{13}\text{C}_{\text{DHA}}$ s were more isotopically enriched in the DHA-fed animals when compared with the ALA-fed group across all tissues. Each data point represents one animal; solid and dashed lines indicate the mean values for DHA and ALA diets, respectively ( $n = 5$ –6 per group). Data were compared by two-way ANOVA for the interaction of diet and generation; results are presented within each figure. A Bonferroni multiple-comparisons test was conducted following a significant ( $P < 0.05$ ) interaction. <sup>a</sup>A significant difference between diet groups within a generation. <sup>#</sup>A significant difference between generation on the same diet. The upper and lower dotted lines indicate the  $\delta^{13}\text{C}$  signature of dietary DHA and ALA, respectively. The dashed line represents the  $\delta^{13}\text{C}$  of baseline animals; the gray band indicates  $\pm$ SD.

hypothesize that the absence of any generational effect in the ALA diet group is driven by a suspected smaller DHA adipose store following lactation. A smaller peripheral DHA pool reflecting the maternal  $\delta^{13}\text{C}$  signature would then be exhausted more rapidly and, thus, be less pronounced in the brain DHA pool during adulthood.

Despite dietary  $\delta^{13}\text{C}_{\text{LNA}}$  and liver and RBC  $\delta^{13}\text{C}_{\text{ARA}}$  signatures being similar, we found serum  $\delta^{13}\text{C}_{\text{ARA}}$  signatures to differ with respect to dietary exposures. While we cannot rule out the contribution of the acute appearance of dietary ARA contamination ( $\leq 0.04\%$  of total FA) from the DHA diet contributing to the observed dietary effect, this result may be driven by differences in long-chain PUFA metabolism between dietary groups. Both mRNA and enzyme activity of delta-5 desaturase and delta-6 desaturase are lower in rodents fed diets containing preformed DHA (46–48). Although we did not directly measure enzyme activity, the approximately 600 nmol/ml lower serum ARA concentration in the DHA diet group, despite diets containing similar levels of LNA, could be explained by reduction in desaturase activity. Alterations in PUFA metabolism resulting from dietary treatments are predicted to contribute to kinetic fractionation effects, which are explained by the consistent  $0.6\text{‰}$   $^{13}\text{C}$  enrichment in serum ARA in the DHA diet group. Alternatively, the isotopic enrichment of

ARA in the DHA group may result from carbon recycling of DHA into ARA through the acetate pool (49); however, we did not detect any evidence of recycling into any saturated or monounsaturated FA pools, nor did we find any other dietary interactions with respect to tissue  $\delta^{13}\text{C}_{\text{ARA}}$ . Therefore, another explanation may be that there are differences in isotope discrimination during the mobilization of ARA into the serum FA pool from either hepatic or adipose stores between groups. Our results demonstrate the power and sensitivity of CSIA for identifying potential subtle differences in metabolic pathways, and the application of this methodology in studying FA metabolism should be explored in greater detail.

The present study demonstrates that the synthesis and incorporation of brain DHA and ARA from 18-carbon essential FAs results in a positive enrichment of  $^{13}\text{C}$  (Fig. 7). Similarly, Rhee, Reed, and Brenna (22) reported that serum ARA  $\delta^{13}\text{C}$  signatures in humans on controlled diets for 8 weeks were more enriched in  $^{13}\text{C}$  than dietary LNA; however, it is not clear whether there was any dietary ARA contribution, as dietary ARA  $\delta^{13}\text{C}$  signatures were not reported.  $\beta$ -Oxidation has been reported to favor isotopically lighter substrate (50), thereby leaving the more enriched FA for incorporation into tissue; however, this phenomena likely did not contribute to the observed enrichment of brain



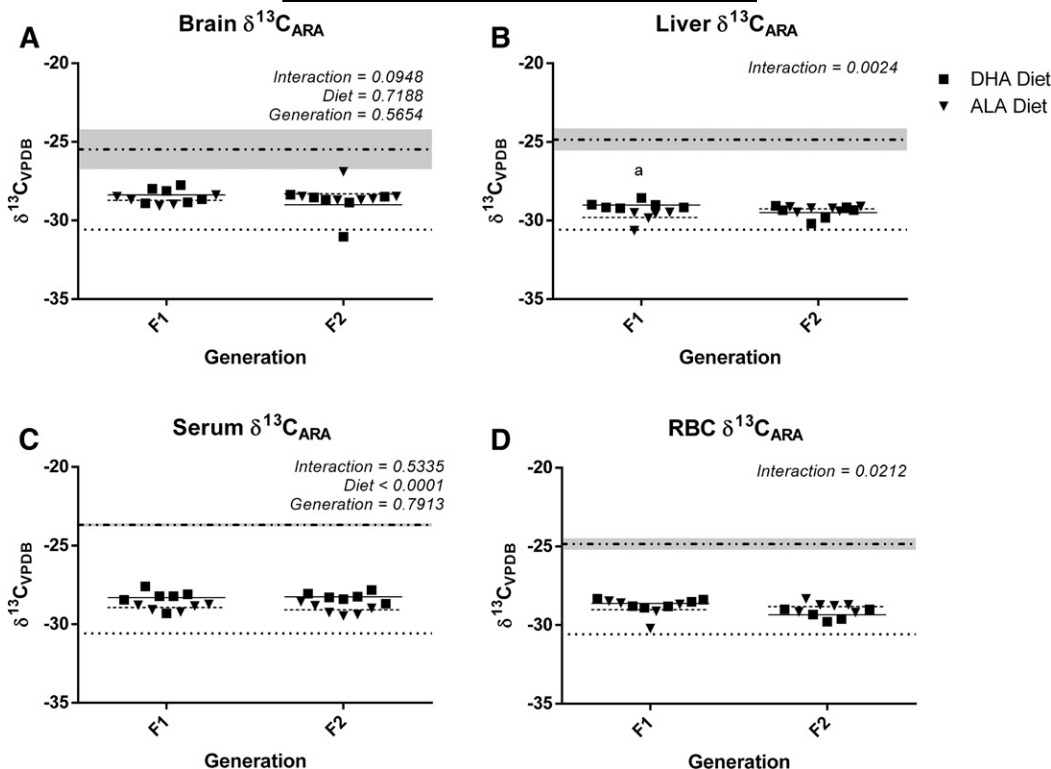


**Fig. 6.** ARA carbon isotope signatures of mice maintained on purified n-3 PUFA-containing diets over multiple generations. Brain (A), liver (B), serum (C), and RBC (D)  $\delta^{13}\text{C}_{\text{ARA}}$ s were found to be similar between dietary groups. Serum  $\delta^{13}\text{C}_{\text{ARA}}$  was more enriched in mice fed the DHA diet. Each data point represents one animal; solid and dashed lines indicate the mean values for DHA and ALA diets, respectively ( $n = 5\text{--}6$  per group). Data were compared by two-way ANOVA for the interaction of diet and generation; results are presented within each figure. A Bonferroni multiple-comparisons test was conducted following a significant ( $P < 0.05$ ) interaction. <sup>a</sup>A significant difference between diet groups within a generation. The dotted line indicates the  $\delta^{13}\text{C}$  signature of dietary LNA. The dashed line represents the  $\delta^{13}\text{C}$  of baseline animals; the gray band indicates  $\pm$ SD.

DHA and ARA over dietary precursors. This is evidenced by the lack of deviation of the serum and liver LNA  $\delta^{13}\text{C}$  signatures from that of the diet (data not shown). Rather, we hypothesize that the notable enrichment is driven by the elongation of ALA and LNA with carbon moieties derived from dietary carbohydrates, which were isolated from corn, a C4 plant highly enriched in  $^{13}\text{C}$ .

Our data serve to demonstrate the application of CSIA as a useful biomarker of FA intake, and may be specifically relevant to determine DHA intake from fish and marine-based foods and/or supplements. Currently, bulk stable isotope analysis is being used to circumvent the shortfalls of subjective self-reported dietary intakes in cross-sectional and clinical studies looking at added sugar intake (51). The benefits of objective measures of nutrient intake are well-known. With respect to fish oil and DHA intake, researchers often rely on changes in circulating DHA levels, which may be influenced by numerous factors (e.g., sex, genetics, BMI, age, etc.), potentially leading to large inter-personal dose-response variations (52–54). In the present study, we found serum and RBC  $\delta^{13}\text{C}_{\text{DHA}}$  signatures to closely reflect the contribution of respective dietary n-3 PUFAs. This finding may prove  $\delta^{13}\text{C}_{\text{DHA}}$  signatures to be a useful tool when assessing compliance in large clinical trials and to validate self-reported intake data. Future work

should look to validate this measure against changes in DHA blood levels following a dose-response in a heterogeneous population.

CSIA can also be used as a tool to estimate the metabolic turnover of FAs within tissues without the need for stable- or radio-labeled tracers by using a diet-switch experiment (23, 26). By manipulating the dietary  $\delta^{13}\text{C}$  signature and measuring the corresponding changes in tissue FA pools over time, tissue-specific turnover and incorporation kinetics can be calculated. This approach has been used routinely by ecologists at the elemental stable isotope level to determine carbon and protein incorporation dynamics, but has been applied limitedly to study lipid metabolism (14). Demmelmair et al. (23) first adapted the diet-switch approach to newly born infants to estimate the daily synthesis rate of ARA by switching from  $^{13}\text{C}$  deplete mother's milk to a more enriched corn-based formula. Carnielli et al. (26) then used a similar approach to track the synthesis of long-chain PUFAs over 7 months in infants fed a formula with naturally enriched DHA and ARA. An important assumption of applying this technique to study lipid kinetics is that equilibration between slow metabolizing tissue pools is achieved. In this study, we show that, under the current dietary conditions, it is necessary to maintain mice on study diets over multiple generations to equilibrate the brain DHA  $\delta^{13}\text{C}$

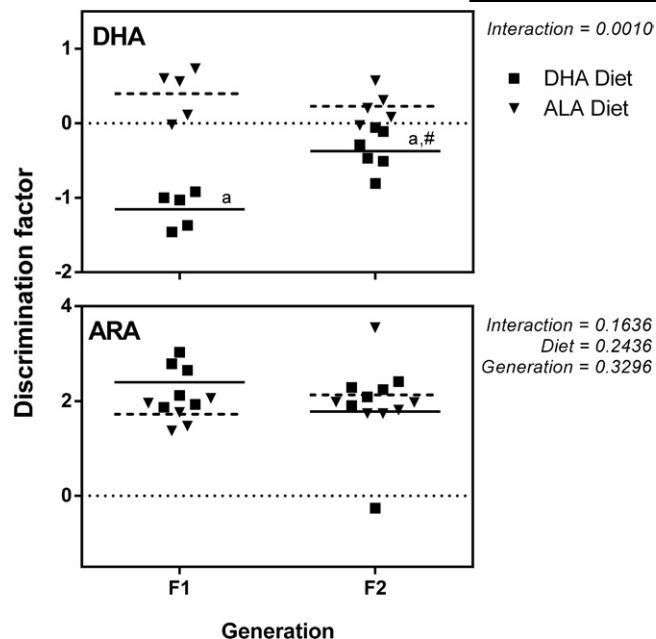


**Fig. 7.** Carbon isotopic discrimination factors calculated for brain DHA and ARA. Data show the enrichment of ARA and DHA derived from 18-carbon precursors over dietary signatures. Each data point represents one animal; solid and dashed lines indicate the mean values for DHA and ALA diets, respectively ( $n = 5-6$  per group). Data were compared by two-way ANOVA for the interaction of diet and generation; results are presented within each figure. A Bonferroni multiple-comparisons test was conducted following a significant ( $P < 0.05$ ) interaction. <sup>a</sup>A significant difference between diet groups within a generation. <sup>#</sup>A significant difference between generation on the same diet.

signature with that of the diet. Ongoing studies in our laboratory plan to use the diet-switch technique in conjunction with CSIA to study the routing and incorporation kinetics of FAs into various tissues following chronic feeding.

Although CSIA presents the unique ability to track the incorporation of dietary FAs into tissue lipid pools, analyte abundance presents some issues when at low concentrations. Our IRMS operated in a linear range between 250 and 10,000 mV. Due to the low relative abundance of DHA in adipose tissue, 0.03–0.09% of FAs in our ALA-fed mice (data not shown), we were unable to achieve consistent  $\delta^{13}\text{C}$  signatures for adipose tissue. Variability and repeatability issues likely manifested due to decreased ionization efficiency at such low abundances of carbon (approximately 0.05–0.15 nmol of carbon per injection). To overcome this issue, it is possible to concentrate low abundance lipids by HPLC prior to CSIA; however, caution must be taken not to inadvertently generate artifacts due to the potential introduction of a kinetic isotope during this step. In the present study,  $\delta^{13}\text{C}$  values for the methylation correction factors were determined by EA-IRMS, which may have the potential to introduce a minor artifact due to any isotopic bias or discrimination that may result from the differential flow paths between the EA- and GC-IRMS. Calibration against the reference  $\text{CO}_2$  with a known  $\delta^{13}\text{C}$  value could overcome this potential issue (55). However, as the  $\delta^{13}\text{C}$  value for the derivatized methyl group is assumed to be uniform

across all FAMES, any potential minor artifacts would not impact between group comparisons.

In conclusion, this study demonstrated the effectiveness of CSIA to differentiate between the incorporation of DHA derived from either preformed marine DHA or terrestrial origin precursor ALA into the brain. Although DHA from either source is indistinguishable by traditional analytical techniques, we demonstrated a clear distinction based on differences in carbon isotopic signatures. The adaptation of this technique for biomarker analysis and use in long-term chronic feeding metabolic studies may prove invaluable as an alternative to the prohibitively expensive administration of chemically synthesized FA tracers. **JLR**

## REFERENCES

- Martinez, M. 1992. Abnormal profiles of polyunsaturated fatty acids in the brain, liver, kidney and retina of patients with peroxisomal disorders. *Brain Res.* **583**: 171–182.
- Taha, A. Y., Y. Cheon, K. Ma, S. I. Rapoport, and J. S. Rao. 2013. Altered fatty acid concentrations in prefrontal cortex of schizophrenic patients. *J. Psychiatr. Res.* **47**: 636–643.
- Bazinet, R. P., and S. Layé. 2014. Polyunsaturated fatty acids and their metabolites in brain function and disease. *Nat. Rev. Neurosci.* **15**: 771–785.
- Liu, J. J., P. Green, J. John Mann, S. I. Rapoport, and M. E. Sublette. 2015. Pathways of polyunsaturated fatty acid utilization: implications for brain function in neuropsychiatric health and disease. *Brain Res.* **1597**: 220–246.
- Kim, H. Y. 2007. Novel metabolism of docosahexaenoic acid in neural cells. *J. Biol. Chem.* **282**: 18661–18665.
- Domenichiello, A. F., A. P. Kitson, and R. P. Bazinet. 2015. Is docosahexaenoic acid synthesis from alpha-linolenic acid sufficient to supply the adult brain? *Prog. Lipid Res.* **59**: 54–66.
- Chen, C. T., A. P. Kitson, K. E. Hopperton, A. F. Domenichiello, M.-O. Trépanier, L. E. Lin, L. Ermini, M. Post, F. Thies, and R. P. Bazinet. 2015. Plasma non-esterified docosahexaenoic acid is the major pool supplying the brain. *Sci. Rep.* **5**: 15791.
- Chen, C. T., Z. Liu, and R. P. Bazinet. 2011. Rapid de-esterification and loss of eicosapentaenoic acid from rat brain phospholipids: an intracerebroventricular study. *J. Neurochem.* **116**: 363–373.
- Lefkowitz, W., S. Y. Lim, Y. Lin, and N. Salem. 2005. Where does the developing brain obtain its docosahexaenoic acid? Relative contributions of dietary alpha-linolenic acid, docosahexaenoic acid, and body stores in the developing rat. *Pediatr. Res.* **57**: 157–165.
- Robinson, P. J., J. Noronha, J. J. DeGeorge, L. M. Freed, T. Nariai, and S. I. Rapoport. 1992. A quantitative method for measuring regional in vivo fatty-acid incorporation into and turnover within brain phospholipids: review and critical analysis. *Brain Res. Brain Res. Rev.* **17**: 187–214.
- Liu, L., N. Bartke, H. Van Daele, P. Lawrence, X. Qin, H. G. Park, K. Kothapalli, A. Windust, J. Bindels, Z. Wang, et al. 2014. Higher efficacy of dietary DHA provided as a phospholipid than as a triglyceride for brain DHA accretion in neonatal piglets. *J. Lipid Res.* **55**: 531–539.
- Kitson, A. P., A. H. Metherell, C. T. Chen, A. F. Domenichiello, M. O. Trpanier, A. Berger, and R. P. Bazinet. 2016. Effect of dietary docosahexaenoic acid (DHA) in phospholipids or triglycerides on brain DHA uptake and accretion. *J. Nutr. Biochem.* **33**: 91–102.
- Sarkadi-Nagy, E., V. Wijendran, G. Y. Diau, A. C. Chao, A. T. Hsieh, A. Turpeinen, P. Lawrence, P. W. Nathanielsz, and J. T. Brenna. 2004. Formula feeding potentiates docosahexaenoic and arachidonic acid biosynthesis in term and preterm baboon neonates. *J. Lipid Res.* **45**: 71–80.
- Wolf, N., S. A. Carleton, and C. Martínez del Río. 2009. Ten years of experimental animal isotopes ecology. *Funct. Ecol.* **23**: 17–26.
- Carleton, S. A., L. Kelly, R. Anderson-Sprecher, and C. Martínez del Río. 2008. Should we use one-, or multi-compartment modes to describe  $^{13}\text{C}$  incorporation into animal tissues? *Rapid Commun. Mass Spectrom.* **22**: 3008–3014.
- O'Brien, D. M., D. P. Schrag, and C. Martínez del Río. 2000. Allocation to reproduction in a hawkmoth: a quantitative analysis using stable carbon isotopes. *Ecology.* **81**: 2822–2831.

17. Tieszen, L. L., T. W. Boutton, K. G. Tesdahl, and N. A. Slade. 1983. Fractionation and turnover of stable carbon isotopes in animal tissues: implications for delta13C analysis of diet. *Oecologia*. **57**: 32–37.
18. Smith, B. N., and S. Epstein. 1971. Two categories of 13C/12C ratios for higher plants. *Plant Physiol.* **47**: 380–384.
19. Nakamura, K., D. Schoeller, F. Winkler, and H. Schmidt. 1982. Geographical variations in the carbon isotope composition of the diet and hair in contemporary man. *Biomed. Mass Spectrom.* **9**: 390–394.
20. Brenna, J. T., T. N. Corso, H. J. Tobias, and R. J. Caimi. 1997. High-precision continuous-flow isotope ratio mass spectrometry. *Mass Spectrom. Rev.* **16**: 227–258.
21. Meier-Augenstein, W. 2002. Stable isotope analysis of fatty acids by gas chromatography-isotope ratio mass spectrometry. *Anal. Chim. Acta.* **465**: 63–79.
22. Rhee, S. K., R. G. Reed, and J. T. Brenna. 1997. Fatty acid carbon isotope ratios in humans on controlled diets. *Lipids*. **32**: 1257–1263.
23. Demmelmair, H., U. v. Schenck, E. Behrendt, T. Sauerwald, and B. Koletzko. 1995. Estimation of arachidonic acid synthesis in full term neonates using natural variation of 13C content. *J. Pediatr. Gastroenterol. Nutr.* **21**: 31–36.
24. McCloy, U., M. A. Ryan, P. B. Pencharz, R. J. Ross, and S. C. Cunnane. 2004. A comparison of the metabolism of eighteen-carbon 13C-unsaturated fatty acids in healthy women. *J. Lipid Res.* **45**: 474–485.
25. Plourde, M., R. Chouinard-Watkins, C. Rioux-Perreault, M. Fortier, M. T. Dang, M. J. Allard, J. Tremblay-Mercier, Y. Zhang, P. Lawrence, M. C. Vohl, et al. 2014. Kinetics of 13C-DHA before and during fish-oil supplementation in healthy older individuals. *Am. J. Clin. Nutr.* **100**: 105–112.
26. Carnielli, V. P., M. Simonato, G. Verlato, I. Luijendijk, M. De Curtis, P. J. J. Sauer, and P. E. Cogo. 2007. Synthesis of long-chain polyunsaturated fatty acids in preterm newborns fed formula with long-chain polyunsaturated fatty acids. *Am. J. Clin. Nutr.* **86**: 1323–1330.
27. Hixson, S. M., C. C. Parrish, and D. M. Anderson. 2014. Changes in tissue lipid and fatty acid composition of farmed rainbow trout in response to dietary camelina oil as a replacement of fish oil. *Lipids*. **49**: 97–111.
28. Richter, E. K., J. E. Spangenberg, M. Kreuzer, and F. Leiber. 2010. Characterization of rapeseed (brassica napus) oils by bulk C, O, H, and fatty acid C stable isotope analyses. *J. Agric. Food Chem.* **58**: 8048–8055.
29. Banerjee, S., T. Kurtis Kyser, A. Vuletich, and E. Leduc. 2015. Elemental and stable isotopic study of sweeteners and edible oils: constraints on food authentication. *J. Food Compos. Anal.* **42**: 98–116.
30. Folch, J., M. Lees, and G. H. Slone Stanley. 1957. A simple method for the isolation and purification of total lipids from animal tissues. *J. Biol. Chem.* **226**: 497–509.
31. Reed, C. F., S. N. Swisher, G. V. Marinetti, and E. G. Eden. 1960. Studies of the lipids of the erythrocyte. I. Quantitative analysis of the lipids of normal human red blood cells. *J. Lab. Clin. Med.* **56**: 281–289.
32. Morrison, W. R., and L. M. Smith. 1964. Preparation of fatty acid methyl esters and dimethylacetals from lipids with boron fluoride-methanol. *J. Lipid Res.* **5**: 600–608.
33. Rieley, G. 1994. Derivatization of organic compounds prior to gas chromatographic-combustion-isotope ratio mass spectrometric analysis: identification of isotope fractionation processes. *Analyst (Lond.)*. **119**: 915–919.
34. Budge, S. M., S. W. Wang, T. E. Hollmen, and M. J. Wooller. 2011. Carbon isotopic fractionation in eider adipose tissue varies with fatty acid structure: implications for trophic studies. *J. Exp. Biol.* **214**: 3790–3800.
35. Goodman, K. J., and J. T. Brenna. 1992. High sensitivity tracer detection using high-precision gas chromatography-combustion isotope ratio mass spectrometry and highly enriched [U-13C]-labeled precursors. *Anal. Chem.* **64**: 1088–1095.
36. Brand, W. A., and T. B. Coplen. 2012. Stable isotope deltas: tiny, yet robust signatures in nature. *Isotopes Environ. Health Stud.* **48**: 393–409.
37. Paul, D., G. Skrzypek, and I. Fórizs. 2007. Normalization of measured stable isotopic compositions to isotope reference scales – a review. *Rapid Commun. Mass Spectrom.* **21**: 3006–3014.
38. Domenichiello, A. F., C. T. Chen, M-O. Trepanier, P. M. Stavro, and R. P. Bazinet. 2014. Whole body synthesis rates of DHA from  $\alpha$ -linolenic acid are greater than brain DHA accretion and uptake rates in adult rats. *J. Lipid Res.* **55**: 62–74.
39. Janssen, C. I. F., V. Zerbi, M. P. C. Mutsaers, B. S. W. de Jong, M. Wiesmann, I. A. C. Arnoldussen, B. Geenen, A. Heerschap, F. A. J. Muskiet, Z. E. Jouni, et al. 2015. Impact of dietary n-3 polyunsaturated fatty acids on cognition, motor skills and hippocampal neurogenesis in developing C57BL/6J mice. *J. Nutr. Biochem.* **26**: 24–35.
40. Moriguchi, T., R. S. Greiner, and N. Salem. 2000. Behavioral deficits associated with dietary induction of decreased brain docosahexaenoic acid concentration. *J. Neurochem.* **75**: 2563–2573.
41. Desai, A., K. Kevala, and H. Y. Kim. 2014. Depletion of brain docosahexaenoic acid impairs recovery from traumatic brain injury. *PLoS One*. **9**: e86472.
42. Moranis, A., J. C. Delpech, V. De Smedt-Peyrusse, A. Aubert, P. Guesnet, M. Lavalie, C. Joffre, and S. Layé. 2012. Long term adequate n-3 polyunsaturated fatty acid diet protects from depressive-like behavior but not from working memory disruption and brain cytokine expression in aged mice. *Brain Behav. Immun.* **26**: 721–731.
43. Kim, H-W., J. S. Rao, S. I. Rapoport, and M. Igarashi. 2011. Regulation of rat brain polyunsaturated fatty acid (PUFA) metabolism during graded dietary n-3 PUFA deprivation. *Prostaglandins Leukot. Essent. Fatty Acids*. **85**: 361–368.
44. DeMar, J. C., C. DiMartino, A. W. Baca, W. Lefkowitz, and N. Salem. 2008. Effect of dietary docosahexaenoic acid on biosynthesis of docosahexaenoic acid from alpha-linolenic acid in young rats. *J. Lipid Res.* **49**: 1963–1980.
45. Oosting, A., H. J. Verkade, D. Kegler, B. J. M. van de Heijning, and E. M. van der Beek. 2015. Rapid and selective manipulation of milk fatty acid composition in mice through the maternal diet during lactation. *J. Nutr. Sci.* **4**: e19.
46. Cho, H. P., M. Nakamura, and S. D. Clarke. 1999. Cloning, expression, and fatty acid regulation of the human delta-5 desaturase. *J. Biol. Chem.* **274**: 37335–37339.
47. Cho, H. P., M. T. Nakamura, and S. D. Clarke. 1999. Cloning, expression, and nutritional regulation of the mammalian delta-6 desaturase. *J. Biol. Chem.* **274**: 471–477.
48. Nakamura, M. T., and T. Y. Nara. 2003. Essential fatty acid synthesis and its regulation in mammals. *Prostaglandins Leukot. Essent. Fatty Acids*. **68**: 145–150.
49. Sheaff Greiner, R. C., Q. Zhang, K. J. Goodman, D. A. Giussani, P. W. Nathanielsz, and J. T. Brenna. 1996. Linoleate, alpha-linolenate, and docosahexaenoate recycling into saturated and monounsaturated fatty acids is a major pathway in pregnant or lactating adults and fetal or infant rhesus monkeys. *J. Lipid Res.* **37**: 2675–2686.
50. DeNiro, M. J., and S. Epstein. 1978. Influence of diet on the distribution of carbon isotopes in animals. *Geochim. Cosmochim. Acta.* **42**: 495–506.
51. Davy, B., and H. Jahren. 2016. New markers of dietary added sugar intake. *Curr. Opin. Clin. Nutr. Metab. Care*. **19**: 282–288.
52. Rice, H. B., A. Bernasconi, K. C. Maki, W. S. Harris, C. von Schacky, and P. C. Calder. 2016. Conducting omega-3 clinical trials with cardiovascular outcomes: proceedings of a workshop held at ISSFAL 2014. *Prostaglandins Leukot. Essent. Fatty Acids*. **107**: 30–42.
53. Browning, L. M., C. G. Walker, A. P. Mander, A. L. West, J. Madden, J. M. Gambell, S. Young, L. Wang, S. A. Jebb, and P. C. Calder. 2012. Incorporation of eicosapentaenoic and docosahexaenoic acids into lipid pools when given as supplements providing doses equivalent to typical intakes of oily fish. *Am. J. Clin. Nutr.* **96**: 748–758.
54. Flock, M. R., A. C. Skulas-Ray, W. S. Harris, T. D. Etherton, J. A. Fleming, and P. M. Kris-Etherton. 2013. Determinants of erythrocyte omega-3 fatty acid content in response to fish oil supplementation: a dose-response randomized controlled trial. *J. Am. Heart Assoc.* **2**: e000513.
55. Zhang, Y., H. J. Tobias, and J. T. Brenna. 2009. Steroid isotopic standards for gas chromatography-combustion isotope ratio mass spectrometry (GCC-IRMS). *Steroids*. **74**: 369–378.